Determination of hyperfine field distributions in amorphous magnets

2006 J. Phys.: Condens. Matter 18 7751

(http://iopscience.iop.org/0953-8984/18/32/022)

INSTITUTE OF PHYSICS PUBLISHING JOURNAL OF PHYSICS: CONDENSED MATTER

J. Phys.: Condens. Matter **18** (2006) 7751–7759 doi:10.1088/0953-8984/18/32/022

Determination of hyperfine field distributions in amorphous magnets

P M Bentley[1] **and S H Kilcoyne**[2]

[1] Hahn-Meitner Institut, Glienicker Straße 100, D-14109 Berlin, Germany
[2] Institute for Materials Research, University of Salford, Salford, M5 4WT, UK

E-mail: phillip.bentley@hmi.de and S.H.Kilcoyne@salford.ac.uk

Received 25 May 2006, in final form 11 July 2006
Published 31 July 2006
Online at stacks.iop.org/JPhysCM/18/7751

Abstract

We present an overview of two leading methods of determining probability distributions from Mössbauer spectra, using the model amorphous magnet $Fe_{80}B_{20}$. A comparison is made between the maximum-entropy method, which permits analysis using truly arbitrary parameter probability distributions, and a Voigtian-based analysis, which uses a sum of Gaussian components to create parameter distributions of pseudo-arbitrary shape. Our results indicate that, in $Fe_{80}B_{20}$, a Gaussian distribution of magnetic hyperfine fields is a very good approximation, although small deviations from a Gaussian shape are evident. We find that the apparent existence of correlations between the isomer shift and magnetic hyperfine field parameters, as found using Voigt-based analyses, may be an artefact of imposing a Gaussian shape on the parameter distributions. We conclude that maximum entropy and Voigtian analyses together provide a very powerful means of characterizing magnetic materials with Mössbauer spectroscopy.

(Some figures in this article are in colour only in the electronic version)

1. Introduction

After the discovery of the Mössbauer effect [1–3], Mössbauer spectroscopy—and in particular ^{57}Fe Mössbauer spectroscopy—quickly developed into an extremely useful scientific probe of magnetic materials. The technique directly measures the splitting of nuclear energy levels, which provides information at a very high resolution about the mean size of the magnetic hyperfine field and the electric field gradient at the Fe nuclear sites. In a simple, homogeneous, ferromagnetic system, a least-squares non-linear regression analysis can be used to fit absorption line shapes to the data. Statements can then be made about the size of the magnetic hyperfine field at the Fe sites with some certainty.

Disordered magnetic materials, such as metallic glasses, may have a range of different hyperfine field environments at the Fe nuclear sites, effectively giving a continuous distribution of fields. In these systems, the analysis becomes somewhat less straightforward. It is widely accepted that the distributions are close to a Gaussian shape. On the other hand, determining the hyperfine field distribution from Mössbauer spectra is a typical 'badly posed' problem involving noisy data, and the number of models consistent with such a given data set is very large. In badly posed problems, simply inverting the transform matrix, which maps a parameter probability distribution onto an instrumental spectrum, produces an unacceptable level of noise in the solution. We therefore need some other means of choosing one of the many available models that offer a good description of the data. By a good description, we mean that the traditional measure of quality of fit, the normalized χ^2 statistic, should equal unity:

$$\chi^2 = \frac{1}{N}\sum_{j=1}^{N}\frac{|y_j - D_j|^2}{\sigma_j^2} = 1 \tag{1}$$

where D are the measured data, σ are the uncertainties, y are the fitted points generated from the model, and N is the number of data points in the spectrum.

Much progress was made in the 1980s regarding this problem. In the first instance, a coarse histogram can be constructed from sub-spectra, using a least-squares non-linear regression-based analysis. Convincing arguments, based on the number of atoms in the first near-neighbour shell, have been used to justify the number of sub-spectra used in such analyses [4] although the data analysis itself is not so satisfactory. A Fourier-series technique also exists [5], which was used previously to study the same model system [6], but this suffers from the drawbacks of imposing symmetrical line intensities onto the spectra (which are generally asymmetric) and introducing oscillations into the probability distribution. The asymmetry in the Mössbauer spectra, i.e. the difference in absorption line intensity on each side of the spectrum, has been attributed to two well documented phenomena. Lines and Eibschütz explain the asymmetry in the Mössbauer spectra from amorphous alloys by the existence of correlations between the hyperfine parameter distributions [7]. Le Caër and Dubois found that the spectral asymmetry is more likely to be brought about the presence of anisotropic dipolar hyperfine fields [8]. As will be shown below, the present study supports the latter view in that we find no evidence for parameter correlations in our analysis. The existing techniques impose a shape—either directly or indirectly—upon the obtained hyperfine field distributions. We would like to be able to select a model that conforms to equation (1) without using such assumptions, and in so doing remove the necessity of a parameter correlation to provide this asymmetry.

The method of maximum entropy (MaxEnt) produces a probability distribution that is maximally non-committal with regard for missing information. In other words, the maximum entropy model is one which satisfies equation (1) whilst using the least amount of required information in the solution. Tests of a MaxEnt algorithm with synthetic Mössbauer spectra (with noise) proved very successful and extremely sensitive to the distribution shape [9, 10].

In light of these advances in magnetic hyperfine field distribution determination from Mössbauer spectra, we consider it timely to compare two of the leading methods of analysis, namely MaxEnt and Voigt-based least-squares regression, and use them to address the question of whether the magnetic hyperfine field is indeed a Gaussian distribution in a model amorphous magnetic system. We will show that in $Fe_{80}B_{20}$ it is a reasonable approximation to model the hyperfine field distributions with correlated Gaussian probability curves. However, we also show that the MaxEnt analysis uncovers deviations from Gaussian behaviour, and that the apparent distribution correlations could be an artefact which results from imposing Gaussian probability curves on the data in the extended Voigt-based fitting technique.

Table 1. Values of the vector elements of β^{h} and β^{ϵ} for a Zeeman-split Mössbauer spectrum.

Line	1	2	3	4	5	6
β^{h}	−0.161 36	−0.093 435	−0.025 51	0.025 51	0.093 435	0.161 36
β^{ϵ}	1	−1	−1	−1	−1	1

2. Experimental details

An ingot containing the appropriate quantities of Fe and B to make $Fe_{80}B_{20}$ was prepared from high purity (>99.99%) elemental materials using an argon-arc furnace. The ingot was then melted using an RF field and projected under an argon atmosphere onto a spinning copper wheel. Typically, a thin amorphous ribbon is produced that measures 2–3 m in length and several hundred microns in thickness. X-ray diffraction confirmed that there were no crystalline impurity phases.

Pieces of ribbon were cut into short lengths, measuring 1–2 cm in length. These pieces were then arranged to form a disc ∼2 cm in diameter and one ribbon thick. Mössbauer spectra were collected at room temperature (∼20 °C) on a conventional, sinusoidal drive, ^{57}Co spectrometer. The data were calibrated for velocity against a spectrum collected at room temperature from pure Fe foil.

3. Data analysis techniques

3.1. Extended Voigt-based fitting

This data analysis technique is part of the commercial software package Recoil [11]. The method has been described fully by the software authors in a previous article [12], so we will only summarize the method here.

One begins by assuming that a Zeeman-split Mössbauer spectrum, *in the static limit*, is comprised of six absorption lines, where each line is described by a Lorentzian function of full width at half maximum γ:

$$L(v_j, v_l, \gamma) = \frac{1}{2\pi} \frac{\gamma}{(v_j - v_l)^2 + (\gamma/2)^2} \tag{2}$$

and where v_j is the velocity at the jth datum point, and v_l is the centre position of the lth absorption line. The six line positions are given by

$$v_l = \beta_l^{\mathrm{h}} H + \beta_l^{\epsilon} \epsilon + \delta \tag{3}$$

where H is the magnetic hyperfine field, and δ is the isomer shift. β^{h} are the velocity shifts per unit magnetic hyperfine field (relative to a pure Fe standard), and β^{ϵ} are the velocity shifts caused by a finite quadrupole shift parameter ϵ, which arises in the presence of an electric field gradient at the absorbing Fe nucleus. Equation (3) originates from a first order perturbation theory, and the validity of the use of this equation will be addressed in section 4. β^{h} and β^{ϵ} for the six spectral lines are given in table 1.

If the sample has distributions of the parameters H, ϵ and δ, instead of single parameter values, then the Mössbauer spectrum is given by a convolution of the Lorentzian-based sextet spectrum with the distribution functions. The resulting absorption spectrum $S(v_l)$ is given by

$$S(v_l) = \sum_{l=1}^{6} a_l \int_{-\infty}^{\infty} \mathrm{d}\delta \int_{-\infty}^{\infty} \mathrm{d}\epsilon \int_{-\infty}^{\infty} P(\delta, \epsilon, H) L(v_j, v_l, \gamma)\, \mathrm{d}H \tag{4}$$

where a_l is the area of the lth line. In the extended Voigt-based fitting method, Lagarec and Rancourt build up a pseudo-arbitrary probability distribution $P(\delta, \epsilon, H)$ using a normalized sum of (correlated) Gaussian components [12], which results in Voigtian absorption line shapes that are approximated by pseudo-Voigtian functions in the software.

3.2. Maximum entropy

The maximum entropy method is an extremely satisfactory means of determining probability distributions from experimental data. It has the advantage that it is not necessary to make assumptions about the shape of $P(\delta, \epsilon, H)$, nor about correlations between the distributions $P(\delta)$, $P(\epsilon)$ and $P(H)$.

A MaxEnt solution has the following favourable qualities.

(i) The probability distribution necessarily contains positive values.
(ii) It is the most uniform solution that is consistent with the data and its errors.
(iii) Any features in the probability distribution that are a departure from uniformity *must* be necessary to describe the data within the experimental uncertainties.

It has been argued that MaxEnt is the *only* method by which probability distributions should be established in the absence of other information, because of the strength of the probability calculus upon which the method is based [13].

We have used an algorithm described by Skilling and Bryan [14], which has proven to be very useful in deconvoluting astronomy data, which was its original purpose. Thereafter, in condensed matter science, it has been used in spectral analysis in transverse-field muon spin rotation experiments [15], in establishing probability distributions of scattering particle sizes in small-angle neutron scattering [16], and in crystallographic applications [17]. Whereas a Bayesian algorithm was used to good effect by Dou [18] in determining the distribution of quadrupole splitting in Fe^{3+}-chlorite, Dou's method differs from our implementation—which is essentially the same as that used by Brand and Le Caër [9]. Dou *et al* use Bayesian methods to establish the prior probability distribution given that the solution must possess finite second derivatives. However, we wish to obtain a smooth probability distribution from the data without forcing this in any way. A smooth probability distribution is produced naturally by the traditional MaxEnt method unless the data justify a departure from smoothness.

The use of the Skilling–Bryan MaxEnt algorithm has already been described several times before (e.g. [15]), so in this paper we present only a short description regarding our implementation (written in C/C++) to analyse Mössbauer spectroscopy.

The problem solved by MaxEnt is the reconstruction of a probability vector f. f is related to the measured data D via the equation

$$D_j = \sum_{i=1}^{K} O_{ji} f_i + \sigma_j \tag{5}$$

where K is the number of elements in the array f, and σ_j is the Gaussian noise on the jth data point. It should be clear from equation (5) why the noise σ prevents a simple inversion of O_{ji} from producing a satisfactory spectrum f. The Skilling–Bryan algorithm uses the *transpose* of O_{ji}, and not the inverse. Indeed, O_{ji}^{-1} need not even exist.

The algorithm searches for an image f which satisfies $\chi^2 = 1$ whilst maximizing the statistical entropy:

$$S = -\sum_{i=1}^{K} p_i \ln\left(\frac{p_i}{w_i}\right) \tag{6}$$

where p is a vector of normalized, weighted probability calculated from f by

$$p_i = \frac{w_i f_i}{\sum_{j=1}^{K} w_j f_j} \tag{7}$$

where w are the weights assigned to each probability f. Because we wish to introduce no prior information into the solution, we set all $w_i = 1$. The solution probability map therefore only contains information that is justified by the data.

We have used MaxEnt to reconstruct a 3D probability map of $P(\delta, \epsilon, H)$, *neither assuming analytical forms for the probability distributions nor any correlation between them*. The transform matrix O_{ji} produces a gamma-ray photon absorption spectrum relative to a flat background level, and is calculated using the following method:

$$O_{ji} = -S(v_j, \alpha_i) \tag{8}$$

where $S(v_j, \alpha_i)$ are Mössbauer sub-spectra. Here we have used α to denote a point in (δ, ϵ, H) parameter space.

In the static limit, the spectrum $S(v_j, \alpha_i)$, with a non-zero magnetic hyperfine field, is an absorption spectrum with six lines, where each line is well described by a Lorentzian function. We therefore have

$$S(v_j) = \sum_{l=1}^{l=6} \eta_l L(v_j, v_l, \gamma) \tag{9}$$

where v_l is determined using the δ, ϵ and H values at point α. η_l, $L(\,)$ and v_l are exactly the same as those in equations (2)–(4).

Depending on the desired resolution of the probability map, the operations on O_{ji} can become reasonably large. In this specific example ($512.64^3 = 134M$ matrix elements, requiring over 500 MB of memory), we required approximately one-and-a-half hours of calculation time on a 1.5 GHz PowerPC processor. Even with moderately sized transform matrices, on modern computing equipment these algorithms are not slow to use—they are much faster than the data acquisition.

We thoroughly tested this software using synthetic data sets of varying degrees of complexity and signal-to-noise ratios, and against Fe standard spectra that were used to calibrate the spectrometers. In all cases, the MaxEnt algorithm reconstructed the correct probability maps.

4. Results and discussion

In both analyses, the best results were obtained by fixing the line areas in the ratios 3:3.02:1:1:3.02:3. It was not possible to model the data adequately with the ratios 3:2:1:1:2:3 as would normally be used for a magnetic sample without any magnetic texture or preferred alignment of the atomic moments. A relative area of 3.02(2) for the second and fifth lines was obtained via the Voigtian analysis, and fed into the MaxEnt analysis for a fair comparison of the two techniques. This indicates a tendency of the atomic moments to point in the plane of the ribbons, i.e. perpendicular to the gamma rays, as was found in other studies on these materials (e.g. [4]). The intrinsic Lorentzian line width (FWHM) was fixed at 0.22 mm s^{-1}, the same broadening as was used in the Voigtian analysis. This value is an approximation to the broadening that can be obtained via a more detailed calculation according to Le Caër *et al* [19].

Figure 1 compares the two models with the experimental data. The best Voigt-based fit to the data was obtained using Gaussian distributions of the two parameters δ and H and one non-zero correlation parameter, $\rho_{\delta H}$. The spectral shape, with a slight asymmetry in the

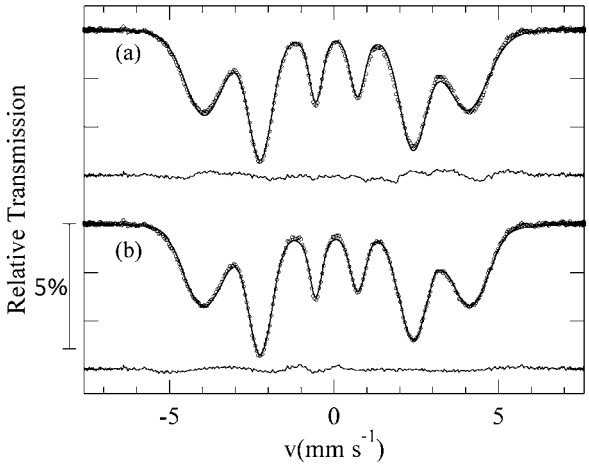

Figure 1. Extended Voigt-based fit (a) and maximum entropy fit (b) to the Mössbauer data of amorphous $Fe_{80}B_{20}$ ribbons. The error bars are smaller than the data points. Beneath each spectrum is also shown the difference between the fits and the data, plotted on the same scale.

Table 2. Results of Voigtian analysis of $Fe_{80}B_{20}$ Mössbauer spectra, assuming that correlations exist between the isomer shift and magnetic hyperfine field distributions.

δ (mm s^{-1})	σ_δ (mm s^{-1})	ϵ (mm s^{-1})	$\mu_0 H$ (T)	$\sigma_{\mu_0 H}$ (T)	$\rho_{\delta H}$
0.067 (3)	0.145 (4)	−0.012 (2)	24.86 (2)	3.34 (2)	0.15 (1)

line intensities, justifies the use of correlations between the parameter distributions. A single value of ϵ was used. Indeed, having a Gaussian distribution of ϵ values made the fit unstable and merely increased the parameter uncertainties by orders of magnitude. In figure 1 there is visually very little to distinguish the quality of the two models, as they offer an adequate description of the experimental data. The misfit statistic χ^2 for the Voigt-based analysis was 2.69, whereas the MaxEnt fit has $\chi^2 = 1$ by definition. The results of the extended Voigt-based fit are summarized in table 2.

The two-dimensional probability map $P(\delta, H)$ obtained from the Voigt-based fit is shown in figure 2. The peak in probability is clearly seen in the centre, at 25 T and 0.07 mm s $^{-1}$. It should also be clear in this figure that the contour lines are not circular, but are instead diagonally distorted, which is caused by the non-zero correlation parameter $\rho_{\delta H} = 0.16(1)$.

The MaxEnt algorithm was used to establish a 3D probability map, covering isomer shifts and quadrupole shifts between -0.9 and 0.9 mm s^{-1}, and covering magnetic hyperfine fields $\mu_0 H$ in the range 0–50 T. The experimental errors were multiplied by a factor of 1.05 to help smooth out the probability distribution and to avoid 'over-analysis' of the data. The mean from ten data points (five from each side of the spectrum) was used as an estimate of the background 100% transmission level. Figure 3 shows the probability matrix $P(\delta, \epsilon, H)$, established by MaxEnt analysis, projected onto the $P(\delta, H)$ plane for comparison with the results from the extended Voigt-based fitting. Again, the probability is strongly peaked in the centre, around 25 T in magnetic hyperfine field and around 0.07 mm s^{-1} in isomer shift. However, figure 3 does not exhibit the same diagonal distortion, and in the centre the contours appear to be more circular in shape. We can therefore conclude that the use of a correlation between the isomer shift and magnetic hyperfine field distributions is not necessarily valid, and may be required in

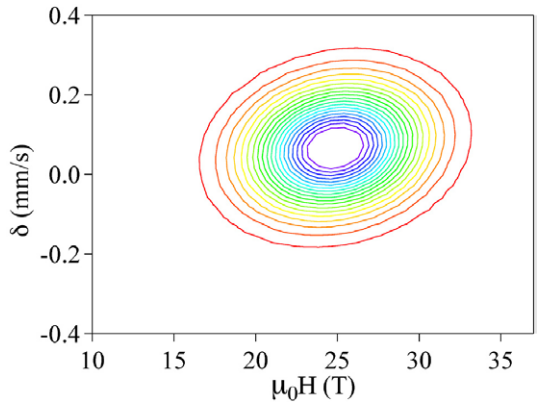

Figure 2. The two-dimensional probability map, as a function of isomer shift and magnetic hyperfine field in $Fe_{80}B_{20}$, determined by extended Voigt-based fitting analysis of the Mössbauer spectrum in figure 1, and allowing correlations between the isomer shift and magnetic hyperfine field distributions. The outermost contour is $p = 0.0002$ and the innermost contour is $p = 0.0022$.

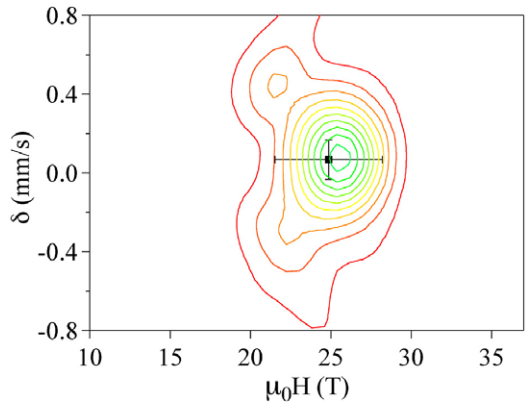

Figure 3. The two-dimensional probability map, as a function of isomer shift and magnetic hyperfine field in $Fe_{80}B_{20}$, determined by MaxEnt analysis of the Mössbauer spectra in figure 1. The outermost contour is $p = 0.0005$ and the innermost contour is $p = 0.004$. For comparison, the Voigtian solution is marked with a black box. The horizontal and vertical bars on the box indicate the width of the Gaussian magnetic hyperfine field distribution, σ_H, and the width of the isomer shift distribution, σ_δ, respectively, obtained by the Voigt-based fitting method.

the Voigt-based fit because of the imposed Gaussian shape on the probability curves. In addition to the broad, central maximum, the MaxEnt analysis reveals lobes of higher-than-background probability centred on $\delta = \pm 0.4$ and at $H \sim 23$ T. The physical significance of this shape in the probability map is currently under investigation.

Averaging the probability density over all isomer shifts δ in figure 3 answers the question 'what is the magnetic hyperfine field distribution at the Fe sites?', which is our main objective in using Mössbauer spectroscopy in such studies on amorphous magnetic samples. The two solutions, obtained from MaxEnt and Voigtian analyses, are shown in figure 4. The two results agree extremely well at low fields, but the MaxEnt solution deviates from the Gaussian shape close to, and above, the peak in $P(H)$. The slight asymmetry in the MaxEnt $P(H)$ curve is also

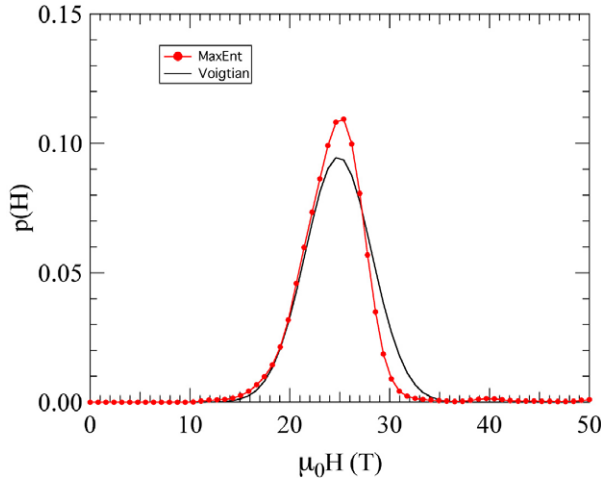

Figure 4. The magnetic hyperfine field probability distributions in $Fe_{80}B_{20}$, obtained as described in the text.

evident in the results obtained by Chien when using the Fourier series method [6], despite the fact that such a Fourier series analysis imposes symmetry on the spectral analysis. So, although the magnetic hyperfine field distribution appears to be nearly Gaussian, we suggest that in reality there may be deviations from a Gaussian shape. The MaxEnt analysis also shows that whilst the distributions $P(\delta)$ and $P(\epsilon)$ are strongly peaked, they also deviate from a Gaussian shape. For the purposes of data analysis, however, the Voigtian and MaxEnt analysis techniques agree to a level such that the Gaussian approximation should not be considered a gross over-simplification. Using the value of mean quadrupole splitting of $\overline{\Delta} = 0.45$ mm s^{-1} from Le Caër *et al* [19] and references therein, and using the parameters $\sigma_H \sim 3.4$ T and $\overline{H} \sim 25$ T from both of these $p(H)$ curves, we find that our results are in good agreement with the previous FeB results plotted on the validity diagram [19]. This indicates that our analysis lies within the region of reliability of first-order perturbation theory, and confirms the validity of the use of the central equation (3) in both of the analysis techniques employed here.

5. Conclusions

We have analysed the magnetic hyperfine field distribution in the model amorphous ferromagnet $Fe_{80}B_{20}$ using both a Voigtian and MaxEnt analysis. We find that the introduction of correlations between the isomer shift and magnetic hyperfine field distributions in the Voigt-based fitting technique produces a good explanation of the data. However, our MaxEnt analysis suggests that this might not be representative of the physics of the material, but may instead be an artefact of the extended Voigt-based fitting technique. Regarding the magnetic hyperfine field distribution itself, we find that it is approximately Gaussian in shape, and the Voigtian analysis offers a rather good approximation with which to model the physical properties of this material. Lastly, we have demonstrated that the combined use of Bayesian and Voigtian analyses of Mössbauer spectra provides a very powerful characterization tool for magnetic samples.

We would like to point out that by extending this technique to several more dimensions in parameter space it should be possible to construct a full, general solution to Mössbauer spectra

based entirely upon probability calculus without prejudice, although the construction of such a model will require much more computational time.

Acknowledgments

We would like to thank Dr N Cowlam (Sheffield, UK) for providing the sample and Dr K Rule (HMI, Berlin, Germany) for very useful discussions. We thank also Professors D Greig and R Cywinski (Leeds, UK) and Dr A Wildes (ILL, Grenoble, France) for helpful discussions and assistance. PMB gratefully acknowledges financial support from the EPSRC and the European Commission (under the Sixth Framework Programme through the Key Action: Strengthening the European Research Area, Research Infrastructures, contract no HII3-CT-2003-505925).

References

[1] Mössbauer R L 1958 *Z. Phys.* **151** 124
[2] Mössbauer R L 1958 *Naturwissenshaften* **45** 538
[3] Mössbauer R L 1959 *Naturforsh.* a **14** 211
[4] Gonser U, Ghafari M and Wagner H G 1978 *J. Magn. Magn. Mater.* **8** 175
[5] Window R 1971 *J. Phys. E: Sci. Instrum.* **4** 401
[6] Chien C L 1978 *Phys. Rev.* B **18** 1003
[7] Lines M E and Eibschütz M 1983 *Solid State Commun.* **45** 435
[8] Le Caër G and Dubois J M 1981 *Phys. Status Solidi* **64** 275
[9] Brand R A and Le Caër G 1988 *Nucl. Instrum. Methods Phys. Res.* B **34** 272
[10] Dobrzyński L, Szymański K and Satuła D 2004 *Nukleonika* **49** s89
[11] Rancourt D G and Lagarec K 1998 Recoil spectral analysis software, www.isapps.ca/recoil
[12] Lagarec K and Rancourt D G 1997 *Nucl. Instrum. Methods Phys. Res.* B **129** 266
[13] Buck B and Macaulay V A (ed) 1991 *Maximum Entropy in Action* (New York: Oxford University Press) chapter 2
[14] Skilling J and Bryan R K 1984 *Mon. Not. R. Astron. Soc.* **211** 111
[15] Rainford B D and Daniel G J 1994 *Hyperfine Interact.* **87** 1129
[16] Jemian P R and Allen A J 1994 *J. Appl. Crystallogr.* **27** 693
[17] Papoular R J, Vekhter Y and Coppens P 1996 *Acta Crystallogr.* A **52** 397
[18] Dou L, Hodgson R J W and Rancourt D G 1995 *Nucl. Instrum. Methods Phys. Res.* B **100** 511
[19] Le Caër G, Dubois J M, Fischer H, Gonser U and Wagner H G 1984 *Nucl. Instrum. Methods Phys. Res.* B **5** 25